

Aberrant expression of AKR1B1 indicates poor prognosis and promotes gastric cancer progression by regulating the AKT-mTOR pathway

Luojie Liu^{1,*}, Lihua Zhu^{1,*}, Zhengwu Cheng², Yibin Sun³, Yuqing Zhou^{3,&}, Jiwei Cao^{4,&}

¹Department of Gastroenterology, Changshu Hospital Affiliated to Soochow University, Suzhou 215501, China

²Department of Gastrointestinal Surgery, The First Affiliated Hospital of Wannan Medical College, Wuhu 241000, China

³Department of Gastroenterology, The Affiliated Suzhou Hospital of Nanjing Medical University, Suzhou Municipal Hospital, Gusu School, Nanjing Medical University, Suzhou, Jiangsu 215005, China

⁴Department of General Surgery, The Affiliated Suzhou Hospital of Nanjing Medical University, Suzhou Municipal Hospital, Gusu School, Nanjing Medical University, Suzhou, Jiangsu 215005, China

*Equal contribution

Correspondence to: Jiwei Cao, Yuqing Zhou; email: jevonskane@126.com, <https://orcid.org/0009-0001-9399-2146>, zyq937065339@163.com, <https://orcid.org/0000-0001-6660-397X>

Keywords: AKR1B1, gastric cancer, prognosis, AKT-mTOR pathway, proliferation and migration

Received: May 23, 2023

Accepted: August 21, 2023

Published: September 24, 2023

Copyright: © 2023 Liu et al. This is an open access article distributed under the terms of the [Creative Commons Attribution License](https://creativecommons.org/licenses/by/3.0/) (CC BY 3.0), which permits unrestricted use, distribution, and reproduction in any medium, provided the original author and source are credited.

ABSTRACT

Gastric cancer (GC) is a common malignant tumor in the digestive tract and a major cause of global cancer death. Due to the limited access to early screening, many patients are diagnosed with advanced GC. Therefore, postoperative radiotherapy and chemotherapy possess limited efficacy in treating GC. AKR1B1 has been associated with tumorigenesis and metastasis across various tumors, becoming a potential therapeutic target for GC. However, its role and mechanism in GC remain unclear. In this study, AKR1B1 was elevated in GC tissue, depicting a poor prognosis. AKR1B1 is closely related to age, vascular and neural invasion, lymph node metastasis, and the TNM stage of GC. The developed survival prediction model suggested that AKR1B1 expression level is crucial in the prognosis of GC patients. Moreover, the expression level of AKR1B1 in GC tissues is closely associated with the AKT-mTOR pathway. *In vitro* and *in vivo* assays functional assays helped determine the oncogenic role of AKR1B1. Additionally, the knockdown of AKR1B1 expression level in GC cell lines could effectively suppress the AKT-mTOR pathway and inhibit the proliferation and migration of tumor cells. In conclusion, this study provides a theoretical basis to establish the potential association and regulatory mechanism of AKR1B1 while offering a new strategy for GC-targeted therapy.

INTRODUCTION

Gastric cancer (GC) is a common malignant tumor in the digestive tract and one of the major causes of global cancer death. [1, 2]. The GC incidence is higher in Asia due to geographic differences, *Helicobacter pylori* infection, and lifestyle factors, including smoking and alcohol consumption. In China, many GC patients have not been actively screened at an early stage, leading to

advanced tumor stages when confirmed [3, 4]. In recent years, continuous progress in surgical techniques and treatment method diversification have effectively elevated survival rate of GC sufferers. Nevertheless, there is a bottleneck in improving the overall treatment effect. Therefore, the key steps to treat GC involve identifying effective diagnostic and therapeutic targets, developing prognostic prediction models, and enhancing therapeutic effects.

Aldo-keto reductases (AKRs) are oxidoreductases which rely on nicotinamide adenine dinucleotide phosphate (NADPH) and are the most glucose reductases. [5, 6]. Aldo-keto reductase 1 member B1 (AKR1B1) is an AKR family member. The space structure of AKR1B1 protein is a single-chain polypeptide, generally existing as a monomer among living biosome. AKR1B1 is able to reversibly bind to NADPH, and the AKR1B1 protein is widely distributed across the human body and is expressed in various tissues and organs [7–9].

The aberrant AKR1B1 protein expression in human tissues has been related to the initiation and progression of various chronic diseases and cancers [7–9]. Studies have demonstrated a causal association between AKR1B1 activity and diabetic complications, such as cataracts, retinopathy, neuropathy, and nephropathy [10, 11]. These chronic diabetes complications are the principal reason for disability or death in such sufferers. In addition, the expression quantity and activity of AKR1B1 protein in human lung cancer, alcoholic liver disease, liver cancer, and breast cancer were significantly elevated and were closely related to tumor progression [6, 9, 12]. Therefore, we focused on the expression changes of AKR1B1 during the occurrence and progression of GC, its relevance with clinical survival and prognosis, and the impact of its aberrant expression on the hyperplasia and metastasis of tumor cells. Thus, our study could provide a new GC-targeted therapeutic strategy with a strong theoretical basis to target AKR1B1 in GC.

MATERIALS AND METHODS

Specimen collection

Our study recruited 115 patients with primary GC and paired contiguous normal stomach tissues after undergoing radical gastrectomy from the First Affiliated Hospital of Wannan Medical College during 2015–2016. Each subject participating in our study signed written informed consent forms. The agreement followed the ethical guidelines set out in the Declaration of Helsinki. The Affiliated Suzhou Hospital of Nanjing Medical University (ID: 2021240) and the institutional review board of the First Affiliated Hospital of Wannan Medical College (ID: 202248) approved this study.

Immunohistochemistry

We fixed the GC specimens and paired contiguous normal stomach tissues with formalin. Then, they were buried in paraffin and cut into 5- μ m slices for immunohistochemical staining as referred in a previous study [13]. Sections were cultured at indoor temperature

for 2 hours using 1:100 diluted anti-AKR1B1 antibody (1:100, Bioss, China). Two blinded researchers evaluated the staining scores to analyze immunohistochemistry (IHC) results. IHC score was decided by the multiple of the intensity (0 as negative; 1 as weak; 2 as moderate; 3 as strong) and extent (0 as 0–5%; 1 as 6–25%; 2 as 26–50%; 3 as 51–75%; 4 as >75%) score. The final point of 0 was considered –; 1–4 considered +; 5–8 considered ++; 9–12 considered +++. In our research, ++ or +++ was deemed to be a positive protein expression, and – or + was considered to be negative.

Cell cultures

The included human GC cell strains were acquired from the Nanjing Medical University (Nanjing, China). They were sprouted in RPMI medium 1640 (Hyclone, USA) with 10% FBS (Gibco, USA), 100 units/ml penicillin G sodium, and 100 μ g/mL streptomycin sulfate (Gibco, USA). The clones were cultivated in 5% CO₂ at 37°C.

Transfection with shRNA

These cells were cultured until 80% fusion and transfected through a lentivirus AKR1B1-shRNA technology (Human AKR1B1-targeting shRNA were procured from GenePharma, China) according to the company's manuals [14]. The cells after transfection were screened using G418 (Roche, Switzerland). Additionally, cell lines with a stable AKR1B1 knock-down were picked for subsequent research.

Protein preparation and western-blot test

The whole proteins were extracted with RIPA lysis buffer comprising proteinase and phosphatase inhibitors (Sigma, USA). The whole protein was separated with SDS-PAGE and shifted to a PVDF membrane which was sealed using 5% skimmed milk and probed using antibodies at 4°C all night long. We visualized the protein bands using chemiluminescence analysis and quantified them with ImageJ (NIH, USA). Antibodies comprised in western-blot were anti-AKR1B1 (1:1000, Bioss, China), anti-p-AKT (1:1000, Cell Signaling Technology, USA), anti-p-S6K1 (1:1000, Cell Signaling Technology, USA), and anti- β -actin (1:1000, Bioss, China) antibodies.

Colony-forming test

About a thousand cells were cultivated in every 6 pore plates for 10 days. The poietic cell lines were fixed by methanol and dyed with 0.1% crystal violet solution. Finally, they were calculated using an optical microscope (Nikon, Japan) equipped with a digicam (Nikon, Japan).

Transwell test

Cells were inoculated into the upper cavities at a density of 10,000 cells/200 μ l in a serum free medium. Each well in the lower cavities was full of complete medium of 800 μ l. After incubation for twelve hours, the filters were fixed using 4% paraformaldehyde and stained by 0.1% crystal violet, and the mean value of 5 random fields in each sample was determined.

Cell viability assay

The GC cell viability was measured with the Cell Counting Kit-8 (CCK-8) test (Abmole Bioscience, USA) in 96-well plates with 2000 cells/well based on the manufacturer's protocols.

Subcutaneous xenograft

SPF male BALB/c naked mice (four weeks, approximately 19 g) were stochastically split into groups, each group of 5. After one week of adaptation, 10^7 AKR1B1-KD or NC-shRNA AGS cells were injected to the right dorsal subcutaneous area of the mice on day 0. Then we measured the weight of mice fortnightly, and the dimensions of their subcutaneous neoplasms was determined. Four weeks later, the subcutaneous neoplasms were peeled and weighed. Ethical clearance by the Animal Ethics Committee of the Affiliated Suzhou Hospital of Nanjing Medical University (Suzhou, China) has been obtained for all the experiments in this study.

Statistical analysis

The data were shown as mean \pm S.D. of a minimum of three stand-alone experiments. Data were analyzed using SPSS 22.0, GraphPad Prism 8, and R software (version 3.6.1). Two groups were compared using the unpaired and two-tailed *t*-test or Mann–Whitney *U* test. The IHC results were analysed using Chi-squared or Fisher's exact tests. $P < 0.05$ was determined statistically significant.

Data availability

Data will be made available on request.

RESULTS

Increased AKR1B1 expression in GC tissues and their association with clinicopathological indicators

Firstly, the AKR1B1 expression was detected in 115 GC tissues and contiguous normal stomach tissues using IHC. The IHC points were decided based on the

intensity and extent of the staining (Figure 1A). The positive AKR1B1 expression levels among normal and cancer gastric cancer tissues were 43.5% and 26.1%, respectively. Based on the IHC scores, there was a high expression of AKR1B1 in GC tissues in contrast to contiguous normal stomach tissues ($P = 0.003$, Figure 1B). What's more, AKR1B1 expression was observably elevated in patients with lymphaden infiltration ($P < 0.001$, Figure 1C) and TNM classification III ($P < 0.001$, Figure 1D).

The staining results were divided into negative and positive based on the IHC score to determine the AKR1B1 expression and its prospective influence in GC tissues. The pertinence between AKR1B1 expression within GC tissues and the clinical pathological indexes of GC patients was assessed. The results suggested AKR1B1 expression was observably correlated with age ($P = 0.044$), vascular invasion ($P = 0.030$), neural infiltration ($P = 0.017$), lymphaden metastasis ($P < 0.001$), and the TNM classification ($P < 0.001$, Table 1). In contrast, no pertinence could be detected between AKR1B1 expression and different clinical pathological indexes ($P > 0.05$, Table 1).

Aberrant expression of AKR1B1 in GC tissues indicates low survival rate

Depending on the close connections between AKR1B1 and clinicopathological indicators, the influence of AKR1B1 expression level was further assessed in GC tissues, affecting the overall survival rate of sufferers. The patients were classified based on AKR1B1^{pos} (AKR1B1 positive) and AKR1B1^{neg} (AKR1B1 negative) expressions. The survival rate of AKR1B1^{pos} sufferers was obviously lower than AKR1B1^{neg} sufferers ($P < 0.001$, Figure 1E). Further subgroup analysis in the light of TNM classification indicated that high AKR1B1 expression determined the low survival rate of sufferers in the stage I-II subgroup ($P = 0.014$, Figure 1F). Nevertheless, AKR1B1 expression was found to be statistically unrelated to overall survival rate in the stage III subgroup ($P = 0.610$, Figure 1G). Thus, AKR1B1 expression could only predict the prognosis of early-stage GC patients instead of an advanced stage.

A subgroup survival analysis was performed according to additional clinical pathological indexes to clarify the predictive effect of AKR1B1 expression on survival across different clinicopathological subgroups. The survival rate of AKR1B1^{pos} patients was markedly lower than AKR1B1^{neg} patients ($P < 0.05$, Figure 2), irrespective of gender, age, differentiated degree, the size of tumor, and vascular and perineural infiltration. Intriguingly, the AKR1B1 expression level did not significantly affect the tumor invasion depth T1-2

($P = 0.050$) or patients with TNM stage III ($P = 0.618$). Conversely, increased AKR1B1 expression was related to worse prognosis in GC patients with the tumor invasion depth T3-4 ($P = 0.021$) or TNM stage I-II ($P = 0.018$). Meanwhile, high AKR1B1 expression could not predict a significant effect on survival, irrespective of whether they belonged to lymph node ($P = 0.097$) or no lymphaden ($P = 0.232$) metastases. Consequently, the AKR1B1 expression level can be detected in GC tissues to evaluate patient survival depending on the clinicopathological indicators.

The single factor analysis of Cox's proportional risk model proved that differentiation degree, vascular invasion, neural invasion, tumor invasion depth, lymphaden metastasis, and AKR1B1 expression ($P < 0.05$, Table 2) are prognosis factors affecting GC patient survival. Lymph node metastasis acted as the

independent factor in the multivariate analysis. Moreover, other indicators, such as AKR1B1 expression, were important in prognosis. By nomograms, we proved the pivotal part of the AKR1B1 expression level in GC to predict post-operative patient survival (Figure 3). The nomograms could forecast the overall survival rate of GC sufferers at 3 and 5 years. The negative or positive AKR1B1 expression could significantly affect the total points, demonstrating the pivotal part of AKR1B1 in forecasting GC patient survival (Figure 3).

Ectopic AKR1B1 regulates the AKT-mTOR pathway to facilitate GC cell migration and proliferation

To gain mechanistic insights into the AKR1B1 effects on GC cell migration and proliferation and the prospective regulatory mechanism of the AKT-mTOR

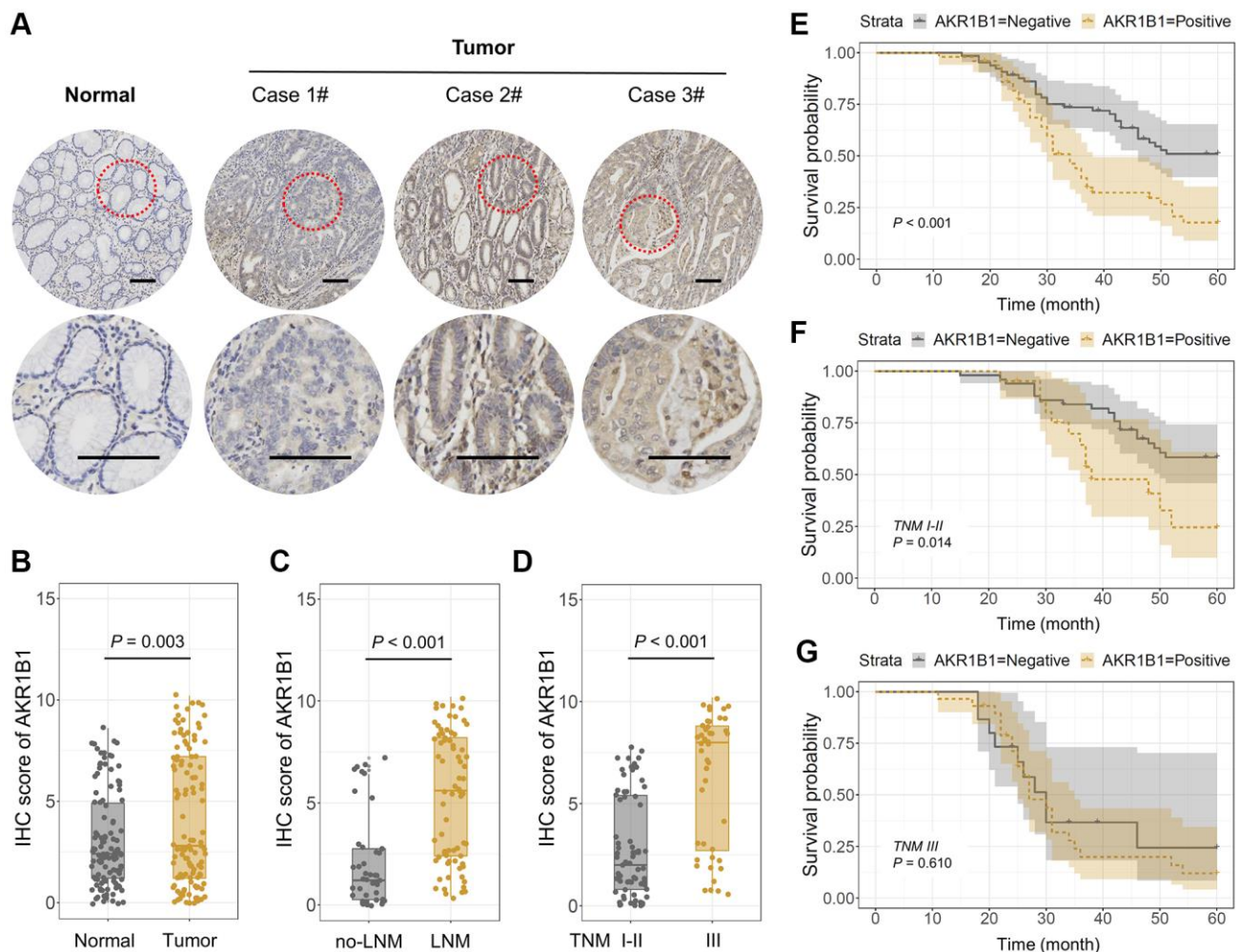


Figure 1. AKR1B1 expression in GC and adjacent normal tissues. (A) The representative IHC images depicting *in situ* AKR1B1 expression in Case 1#, 2#, 3# GC and adjacent normal tissues (scale bar = 100 μ m). (B–E) The IHC scores of AKR1B1 in (B) GC vs. normal tissues, (C) Tumors with or without lymph node metastasis, and (D) TNM stage I–II vs. stage III. (E) The overall survival analysis of AKR1B1^{pos} vs. AKR1B1^{neg} GC patients. (F) In the subgroup of TNM staging I–II, the overall survival analysis of AKR1B1^{pos} vs. AKR1B1^{neg} GC patients. (G) The overall survival analysis of AKR1B1^{pos} vs. AKR1B1^{neg} GC patients in the subgroup of TNM staging III.

Table 1. Association between AKR1B1 and clinic-pathological factors in GC patients.

| Variables | AKR1B1 | | P value |
|---------------------------|----------|----------|---------------------|
| | Negative | Positive | |
| Age (years) | | | |
| <65 | 28 | 31 | 0.044 ^a |
| ≥65 | 37 | 19 | |
| Gender | | | |
| Male | 43 | 37 | 0.365 |
| Female | 22 | 13 | |
| Tumor size (cm) | | | |
| <5 | 48 | 36 | 0.825 |
| ≥5 | 17 | 14 | |
| Degree of differentiation | | | |
| Well | 23 | 11 | 0.119 |
| Poor | 42 | 39 | |
| Vascular invasion | | | |
| Negative | 43 | 23 | 0.030 ^a |
| Positive | 22 | 27 | |
| Neural invasion | | | |
| Negative | 38 | 18 | 0.017 ^a |
| Positive | 27 | 32 | |
| Depth of tumor invasion | | | |
| T1-2 | 27 | 13 | 0.083 |
| T3-4 | 38 | 37 | |
| Lymph node metastasis | | | |
| No | 34 | 8 | <0.001 ^b |
| Yes | 31 | 42 | |
| TNM staging | | | |
| I-II | 50 | 21 | <0.001 ^b |
| III | 15 | 29 | |

^a $P < 0.05$, ^b $P < 0.001$.

pathway, we firstly retrieved AKR1B1 expression in GC clones through the Cancer Cell Line Encyclopedia (CCLE) (Figure 4A, 4B). Whereafter, AKR1B1 expression was detected in GC clones using western blotting, consistent with CCLE platform data (Figure 4C, 4D). Therefore, AGS and MKN45 were selected with high expression of AKR1B1 for transfection with AKR1B1-shRNA and establishment of AKR1B1 knockdown cell lines (AKR1B1-KD). The fluorescence microscope images of AGS and MKN45 cells with control-shRNA and AKR1B1-shRNA transfection were detected to evaluate the knockdown effect (Figure 4E). We also investigated the effect of AKR1B1-KD GC cells with immunoblot, and AKR1B1 knockdown was evident in GC clones (Figure 4F, 4G).

The prospective relevance between AKR1B1 and the AKT-mTOR pathway was analyzed in TCGA datasets

using the GEPIA database. The expression degree of *AKR1B1* in GC tissues had a tight connection with the expression levels of *AKT* ($P = 0.006$) and *mTOR* ($P = 0.014$, Figure 4H). The expression of phosphorylated S6K1 in cancers depicted the AKT-mTOR pathway activation status as a key downstream target. This pathway is crucial in the migration, proliferation, apoptosis, drug resistance, and various abilities of cancer cells [15, 16]. Consequently, we explored the relationship between AKR1B1 expression and phosphorylated AKT and S6K1 using AKR1B1-KD GC cell lines. The outcome was inhibited in AKR1B1-KD GC clones, p-AKT, and p-S6K1 levels (Figure 4I, 4J).

The biology function of AKR1B1 was analysed by AGS and MKN45 knockdown structures. We investigated the multiplication capacity of AKR1B1-KD cells through

Table 2. Results of univariate and multivariate analyses of postoperative patients' survival by Cox's proportional hazard model.

| Varieties | Univariate analysis | | | Multivariate analysis | | |
|--|---------------------|-------------|---------------------|-----------------------|-------------|--------------------|
| | HR | 95% CI | P | HR | 95% CI | P |
| Age (≤60 or >60 years) | 0.913 | 0.563–1.479 | 0.711 | | | |
| Gender (male/female) | 1.349 | 0.777–2.345 | 0.288 | | | |
| Size of tumor (≤5 or >5 cm) | 0.718 | 0.424–1.214 | 0.216 | | | |
| Degree of differentiation (moderate-well/poor) | 0.521 | 0.292–0.929 | 0.027 ^a | 0.650 | 0.361–1.170 | 0.151 |
| Vascular invasion (negative/positive) | 0.424 | 0.260–0.691 | 0.001 ^b | 0.746 | 0.432–1.287 | 0.293 |
| Neural invasion (negative/positive) | 0.433 | 0.262–0.716 | 0.001 ^b | 0.716 | 0.396–1.296 | 0.269 |
| Depth of tumor invasion (T1-2/T3-4) | 0.360 | 0.201–0.645 | 0.001 ^b | 0.631 | 0.314–1.269 | 0.196 |
| Lymph node metastasis (negative/positive) | 0.265 | 0.146–0.482 | <0.001 ^c | 0.437 | 0.219–0.873 | 0.019 ^a |
| AKR1B1 expression (negative/positive) | 0.420 | 0.257–0.686 | 0.001 ^b | 0.651 | 0.388–1.093 | 0.104 |

^a*P* < 0.05, ^b*P* < 0.01, ^c*P* < 0.001.

the CCK-8 and colony-forming assays. Compared with negative controls, the hyperplasia of AKR1B1-KD cells was more markedly repressed (Figure 5A). Agree with these results, the AKR1B1-KD cells similarly exhibited

a poor colony-forming capacity (Figure 5B, 5C). Then, the migration capacity alteration of the AKR1B1-KD cells was evaluated using a transwell assay, which was markedly suppressed (Figure 5D, 5E).

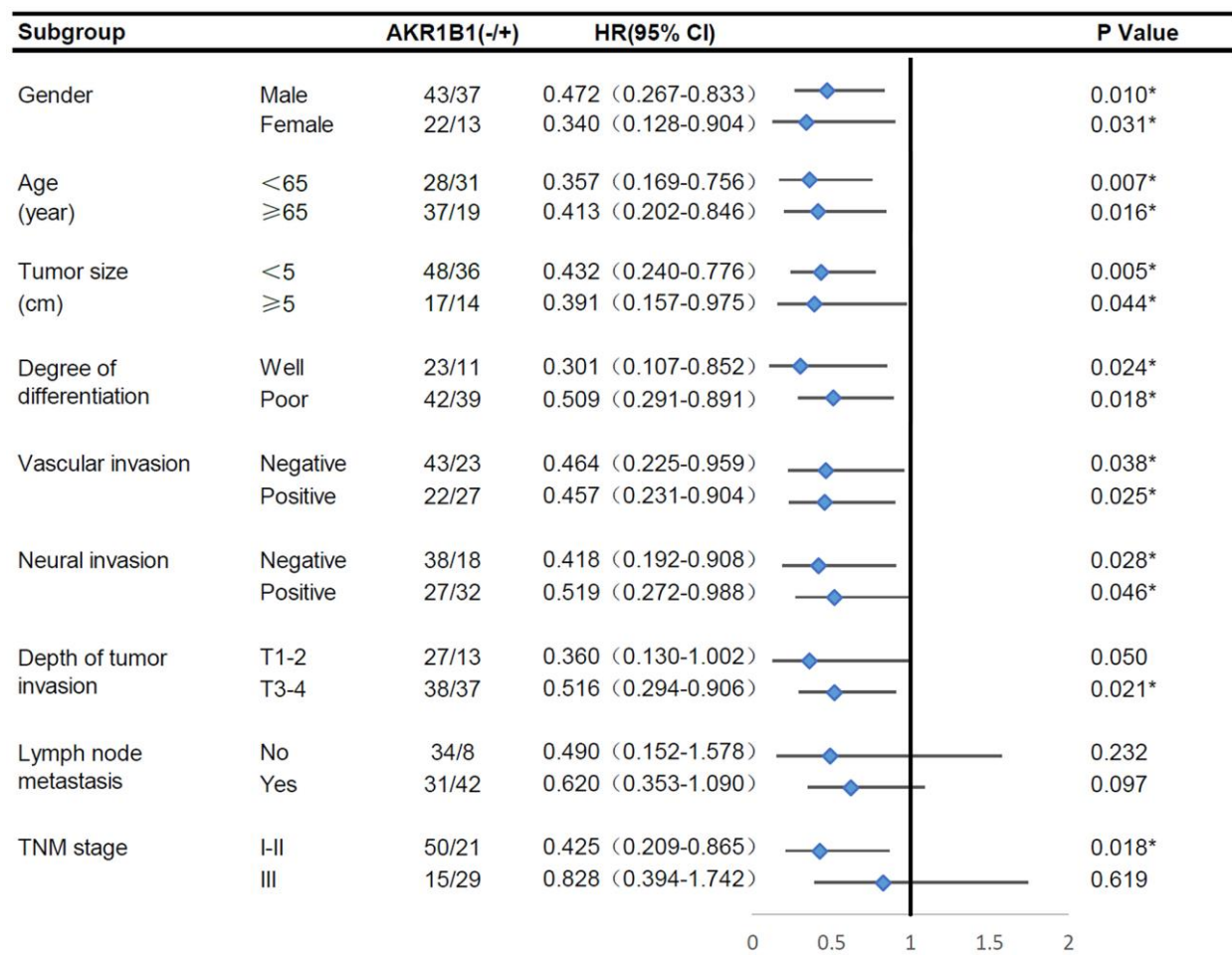


Figure 2. The overall survival analysis of AKR1B1pos vs. AKR1B1neg GC patients in subgroups has been demarcated based on individual clinicopathological indicators.

AKR1B1 promoting tumorigenesis and deteriorating nutrition condition *in vivo*

We built a xenograft murine model using AGS cell lines to demonstrate the AKR1B1 expression level influences on neoplasm growth and nutrition in mice. In contrast to the NC group, the nutrition condition of mice was markedly improved in the AKR1B1-KD group (Figure 6A). Simultaneously, the growth of subcutaneous neoplasms was markedly lowered in the AKR1B1-KD group than that in the NC group (Figure 6B, 6C). The mouse weight was observably influenced by the growth of subcutaneous neoplasms. Additionally, AKR1B1 expression had a vital impact on GC cell hyperplasia and the nutrition condition of mice. Therefore, the

weights of tumor masses were investigated to calculate the net body weight after deducting the respective tumor weights. Observably inhibiting the proliferative capacity of GC cells in the AKR1B1-KD group appeared as reduction of tumor weight and reverse of mouse weight without tumor weight compared with the control group (Figure 6D, 6E).

Furthermore, the AKR1B1 protein expression was detected in subcutaneous tumors with immunoblot. Thus, AKR1B1 expression was more significantly inhibited in the AKR1B1-KD group than in the control group (Figure 6F, 6G). AKR1B1 protein levels were prominently correlated *in situ* with the subcutaneous neoplasm weight (Figure 6H). Then, the cluster analysis

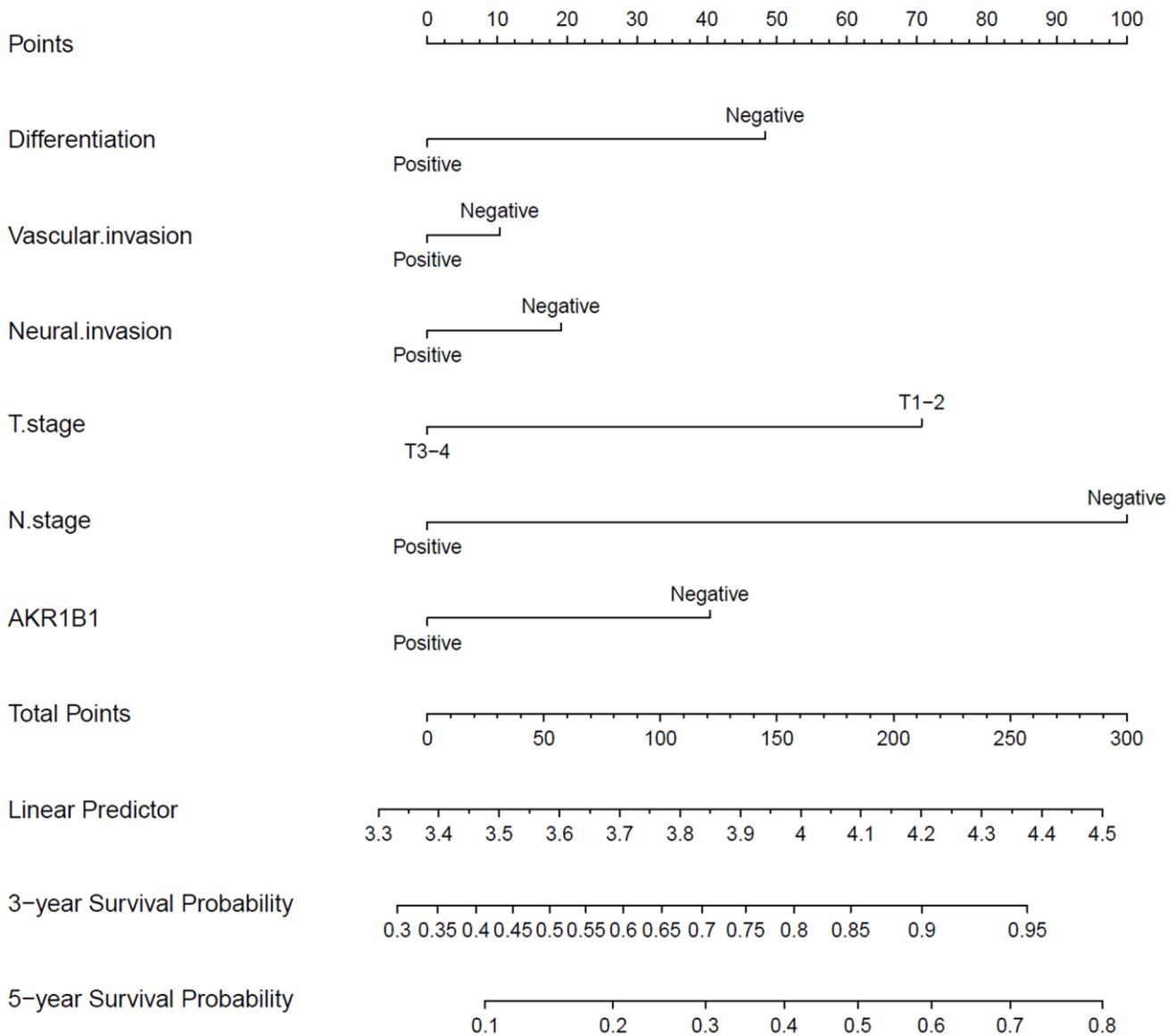


Figure 3. The nomograms for predicting 3- and 5-year overall survival of GC patients. The points of each variable were obtained using a vertical line between each variable and the point scale. The predicted survival rate was connected with the total points through a vertical line drawn from the total points scale to the overall survival.

was performed based on the neoplasm weight and AKR1B1 protein levels. The influence of AKR1B1 expression degree was evaluated on the neoplasm growth in mice (Figure 6I). The results indicated that 20% of the NC group mice and 100% of the AKR1B1-KD group mice belonged to Cluster 1. Moreover, 80% of the NC group mice belonged to Cluster 2 (Figure 6J).

DISCUSSION

GC is a malignant digestive tract tumor possessing high morbidity and mortality [17, 18]. Many patients in China are diagnosed with advanced tumors since active early screening in GC patients is lacking. In recent years, the treatment of GC has considerably improved

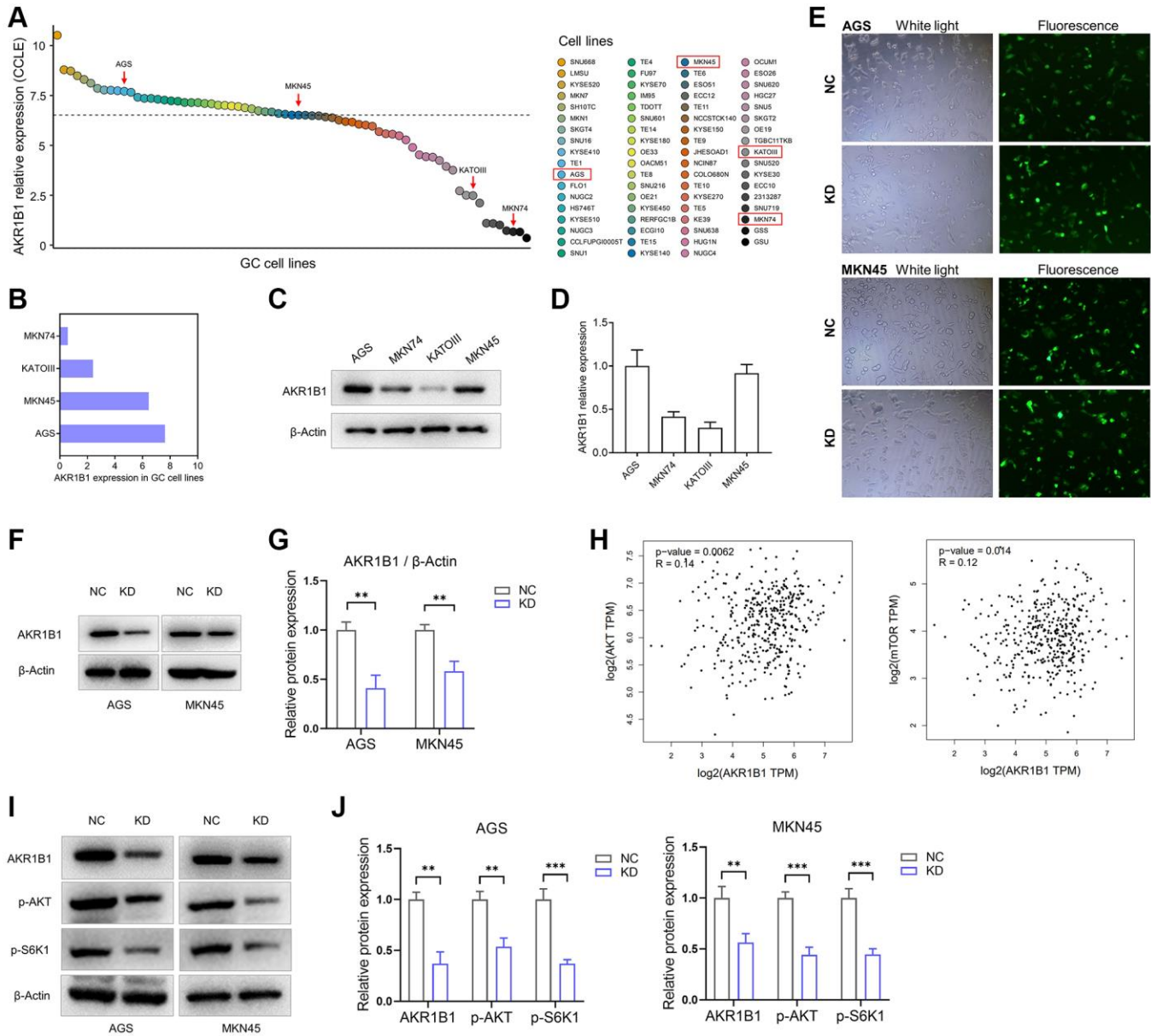


Figure 4. AKR1B1-KD cells were constructed, and the regulatory relationship between AKR1B1 and AKT-mTOR pathway was evaluated. (A) The AKR1B1 expression in GC cell lines was searched from the CCLE platform. (B) The CCLE platform helped select AKR1B1 expression in four GC cell lines. (C) AKR1B1 expression in four GC cell lines was detected using western blotting. (D) The immunoblot result of AKR1B1 expression was semi-quantified in four GC cell lines with ImageJ. (E) The white and fluorescence microscope images of AGS and MKN45 cells were transfected with control-shRNA (NC) and AKR1B1-shRNA (KD). (F) Western blot indicates the AKR1B1 protein levels in NC and AKR1B1-KD AGS and MKN45. (G) The immunoblot results were semi-quantified using ImageJ. (H) The GEPIA platform was used to determine the correlation analysis of *AKR1B1* and *AKT* or *mTOR* gene expression levels in GC patients from TCGA datasets. (I) Western blot reveals the AKR1B1, p-AKT, p-S6K1, and β -actin protein levels in AKR1B1-KD GC cells. (J) The immunoblot results of AGS were semi-quantified using ImageJ. Abbreviations: CCLE: Cancer Cell Line Encyclopedia; NC: negative control; KD: AKR1B1-shRNA. ** $P < 0.01$, *** $P < 0.001$.

with the continuous progress of surgical techniques and the diversification of therapeutic means. However, poor surgical effects and serious chemotherapy resistance are still unavoidable problems for many advanced GC patients [19–21]. Therefore, identifying new targets for diagnosis and treatment while constructing new diagnosis and treatment prediction models are effective strategies for treating GC.

Most AKR family members can perform redox reactions using NADPH, a niacinamide adenine dinucleoside phosphate, as the cofactor. Each AKR family member is a soluble protein with a molecular weight of 34–37 kDa. There are 16 families with more

than 190 members, widely distributed in the prokaryotes and eukaryotes [6, 22]. Meanwhile, many substrates are also present, including chemical carcinogens, fatty aldehydes, carbohydrates, ketone steroids, ketone prostaglandins, and so on. Each family member is similar in protein folding mode with significantly different function [23].

Studies of AKR1B1, an AKR family member, have focused more on diabetes, primarily its association with disease development and complications. Researchers have obtained many AKR1B1 protein inhibitors using biological metabolite extraction or chemical synthesis to utilize them as new clinical drugs for treating diabetic

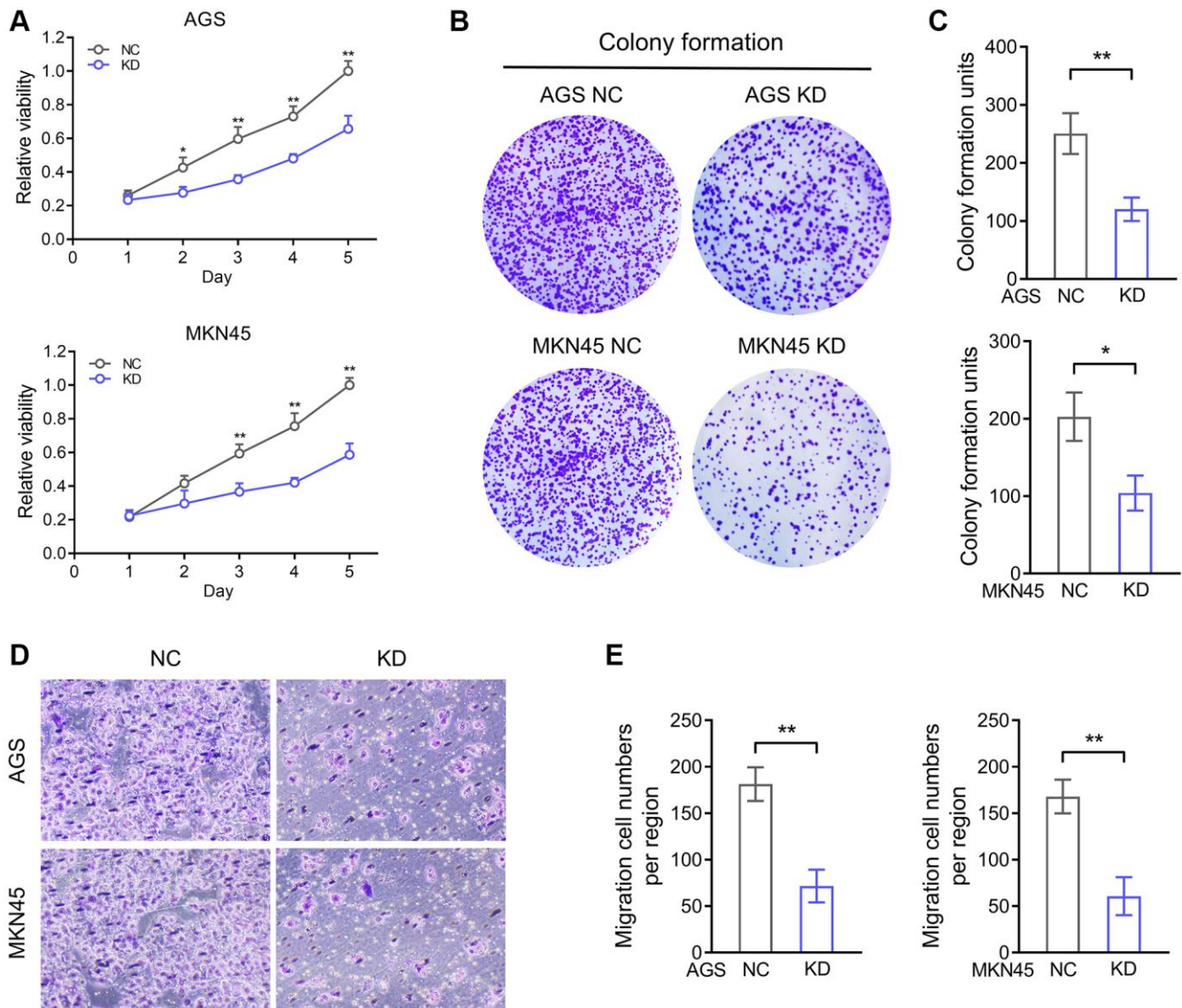


Figure 5. AKR1B1 enhances the proliferation and migration ability of GC cells. (A) The CCK-8 assay determined the proliferation ability of AGS and MKN45 transfecting with AKR1B1-shRNA. (B) The colony formation capacity of AGS and MKN45 transfecting with AKR1B1-shRNA was assessed. (C) The colony-forming units were counted. (D) The migration capacity of AGS and MKN45 transfecting with AKR1B1-shRNA was assessed. (E) The number of migrating cells was counted. Abbreviations: NC: negative control; KD: AKR1B1-shRNA. * $P < 0.05$, ** $P < 0.01$.

complications [24–26]. In recent years, AKR1B1 studies have focused on tumorigenesis correlation. Researchers observed that AKR1B1 expression was

aberrantly increased in malignant tumors, and its expression level affected the survival prognosis of patients [6, 9, 12]. In colorectal carcinoma, the

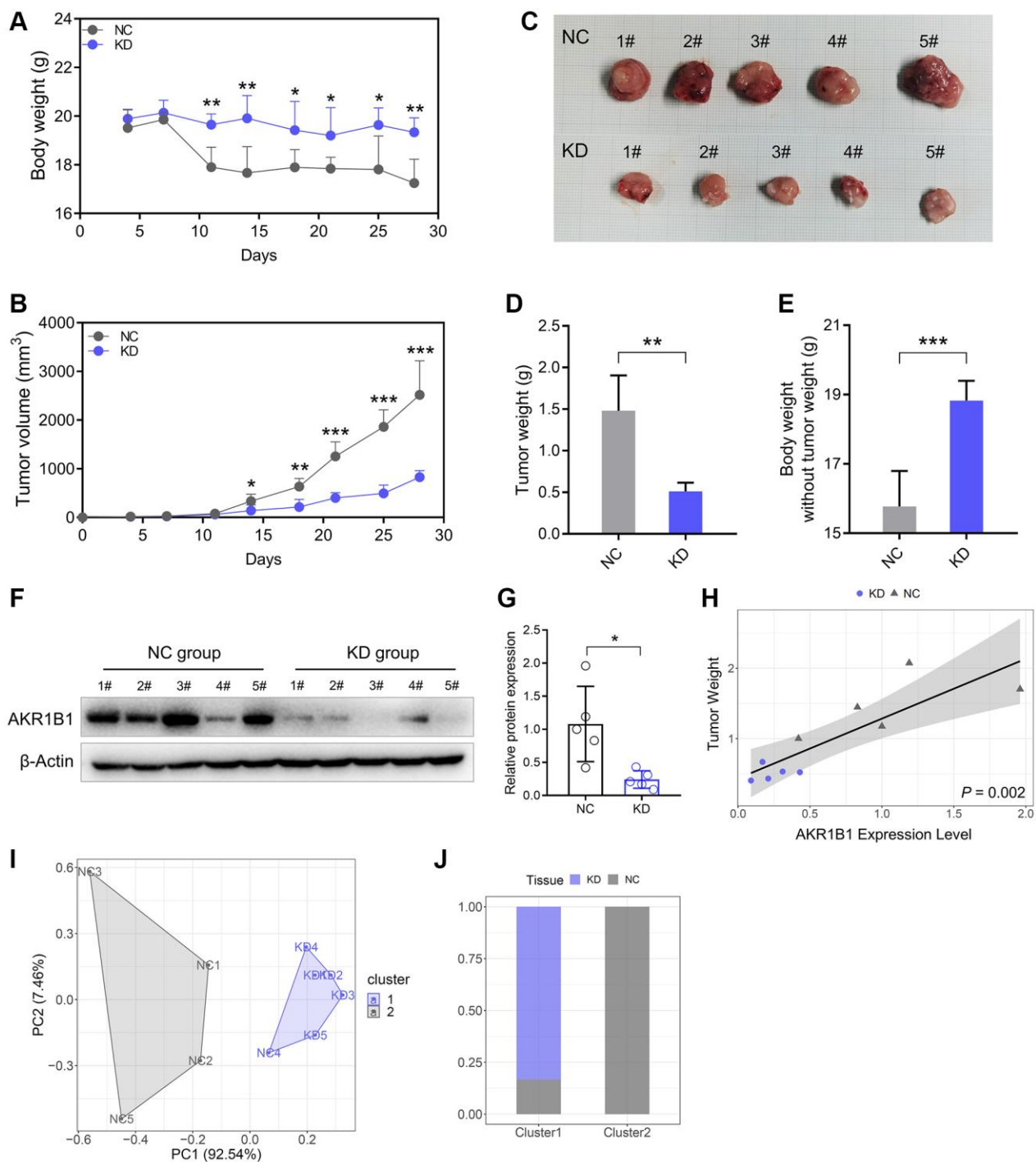


Figure 6. Reduced AKR1B1 inhibits GC tumor growth *in vivo*. (A) During the experiment, the body weight of mice was recorded twice a week. (B) The tumor volume of mice was recorded twice a week during the experiment. (C) The representative images of subcutaneous tumors harvested from NC and AKR1B1-KD groups. (D) The weights of tumor masses. (E) Net body weight after subtracting the respective tumor weights. (F) AKR1B1 expression was detected in subcutaneous tumors using western blotting. (G) The immunoblot result of AKR1B1 expression in subcutaneous tumors was semi-quantified using ImageJ. (H) The association analysis between the AKR1B1 expression levels in tumor tissues and weight. (I) The stratification analysis of mice in Cluster 1 and Cluster 2 depends on the tumor weight and AKR1B1 expression levels. (J) The percentage of NC and AKR1B1-KD mice in each cluster. $n = 5$ for each group. Abbreviations: NC: negative control; KD: AKR1B1-shRNA. * $P < 0.05$, ** $P < 0.01$, *** $P < 0.001$.

AKR1B1 and AKR1B10 expression levels in tumor cells, both AKR family members, and their effect on the proliferation ability of tumor cells showed opposite trends. AKR1B10 was significantly reduced in tumor tissues and cells, and its overexpression could effectively inhibit tumor growth. However, AKR1B1 expression promotes tumor cell proliferation with the colorectal cancer progression [27].

Previous studies have demonstrated that AKR1B1 expression is elevated in GC tissues in contrast to contiguous normal stomach tissues [28]. We performed immunohistochemical staining on 115 GC tissues and paired contiguous normal tissues, and the experimental data showed that AKR1B1 expression was anomalously increased in GC tissues in contrast to paired normal stomach tissues. Furthermore, the AKR1B1 expression level was observably higher in GC tissues of patients with lymphaden metastasis positive or TNM III than those with no lymph node spread or TNM I-II. Therefore, the expression of AKR1B1 in cancerous tissues was elevated with GC tumorigenesis. After tumor formation, the AKR1B1 expression level was further increased with disease progression, which was higher than in early-stage GC tissues. Thus, the progression of GC can be assessed based on AKR1B1 expression. The relationship between AKR1B1 expression and GC progression demonstrated that AKR1B1 can potentially promote the invasion and metastasis of cancerous cells in GC patients.

Additionally, by the correlation analysis between the IHC test of AKR1B1 in GC tissues and the clinical pathological data of GC patients, the AKR1B1 expression was tightly related to the age, lymphaden metastasis, vascular invasion, perineural invasion, and TNM classification of patients. The Kaplan-Meier survival analysis depicted that overexpression of AKR1B1 forecasted poor survival outcomes. Interestingly, the results also demonstrated that high expression of AKR1B1 forecasted poor outcomes in TNM I-II patients. In contrast, AKR1B1 expression had nothing to do with prognosis in TNM III patients. This result was further confirmed in the Cox survival subgroup analysis, depicting the accurate application range of AKR1B1 as a prognostic predictor.

The 3-year or 5-year nomogram analysis depicted that AKR1B1 expression markedly influenced the overall survival rate of GC patients, providing a theoretical foundation for targeted AKR1B1 treatment. The aberrant AKR1B1 expression can potentially affect the biological behavior of tumor cells [29–31]. It has been found that the expression level of AKR1B1 was connected with the EMT process of mammary cancer

cells. Thus, AKR1B1 methylation detected can become a marker for the early breast cancer diagnosis [32]. DNA chip data helped analyze the gene expression profile of drug-resistant hepatocellular carcinoma from nodules to tumor models, indicating the upregulation of the AKR1B1 expression [33]. While studying colorectal cancer using gene enrichment analysis, tumor genome atlas, and RNAseq data, AKR1B1 expression was associated with cell cycle progression, movement, and inflammation [8, 27]. Studies investigating the correlation between AKR1B1 and lung cancer revealed that the AKR1B1 expression change could be significant in the lung cancer metastasis [9]. In addition, AKR1B1 inhibition may play the role of an auxiliary therapy rendering tumor cells more sensitive to anti-tumor therapy or alleviating the untoward reactions [34, 35].

The expression of AKR1B1 was knocked down, and the changes in the migration and proliferation ability of GC cells were analyzed to explore the function of AKR1B1 in GC cells. The findings indicated that the migration and proliferation ability of GC cells was obviously inhibited. We also conducted relevant experiments *in vivo* by constructing subcutaneous tumor model of mice. The tumor was induced by subcutaneous injection of AKR1B1-KD or NC cells. The subcutaneous neoplasm of the AKR1B1-KD group was markedly smaller than that of the NC group. Moreover, the nutrition condition of the AKR1B1-KD group was significantly better than the NC group. The two mice groups could be effectively distinguished using cluster analysis depending on tumor weight and AKR1B1 expression level. Therefore, AKR1B1 expression levels are critical in GC tumorigenesis and growth.

The AKT-mTOR signaling pathway modulates the migration, proliferation, metabolism, and drug resistance of cancer cells [14, 36]. The AKT-mTOR alteration may be affected by MAPK, AMPK, Hedgehog, and other signaling pathways [14, 37, 38]. The TCGA data bank was analysed by the GEPIA platform based on the numerous analogous influences of AKR1B1 and AKT-mTOR on cancer cells. The results revealed that the AKR1B1 gene level had positive correlation with the expression of AKT and mTOR in GC. Meanwhile, the expression of AKR1B1 was reduced, and changes in the phosphorylation level of the AKT-mTOR pathway were detected to demonstrate the regulatory role of AKR1B1 on this pathway at the protein level. The knockdown of AKR1B1 expression in GC cells could efficaciously inhibit AKT and S6K1 phosphorylation, confirming the regulation of the Akt-mTOR pathway by AKR1B1. Khayami et al. considered that the inhibition of

AKR1B1 could decrease the AKT phosphorylation in small bowel and large bowel in *Apc^{Min/+}* mice with a high fat diet. Meanwhile, AKR1B1 inhibition could block the mTOR pathway activation by activating 5' adenosine monophosphate-activated protein kinase (AMPK) as it inhibits the phosphorylation of mTOR, Raptor, eIF4E, S6K, and 4E-BP1, thus inhibiting tumor growth. These regulatory pathways can synthesize the regulatory effects of AKR1B1 on mTOR-related signaling networks [39, 40].

Abnormal elevated expression of AKR1B1 in GC could lead to poor prognosis among GC sufferers. AKR1B1 could be an independent prognostic factor for postoperative GC patients. The prognostic model established according to AKR1B1 expression depicted its considerable impact on patient prognosis. Additionally, *in vitro* and *in vivo* experiments showed that AKR1B1 could accelerate GC cell migration and proliferation ability while affecting the nutritional level by controlling the AKT-mTOR pathway. These findings may provide the theoretical foundation for confirming the prospective connection between AKR1B1 and AKT-mTOR pathway and its regulatory mechanism, providing novel strategies for targeted GC therapy.

AUTHOR CONTRIBUTIONS

Luojie Liu and Lihua Zhu analyzed the data, and wrote the paper. Luojie Liu, Lihua Zhu, Zhengwu Cheng and Yibin Sun performed the experiments. Yuqing Zhou and Jiwei Cao designed the experiments, and provided funding support. All authors read and edited the manuscript.

CONFLICTS OF INTEREST

The authors declare no conflicts of interest related to this study.

ETHICAL STATEMENT AND CONSENT

The study was approved by The Affiliated Suzhou Hospital of Nanjing Medical University (ID: 2021240) and the institutional review board of the First Affiliated Hospital of Wannan Medical College (ID: 202248). The experiments with patients' samples followed the ethical guidelines set out in the Declaration of Helsinki. Each subject participating in our study signed written informed consent forms.

Ethical clearance has been obtained for all animal experiments in this study by the Animal Ethics Committee of the Affiliated Suzhou Hospital of Nanjing Medical University (Suzhou, China).

FUNDING

This study was supported by the Suzhou Special Project of Diagnosis and Treatment for key Clinical Disease (LCZX201814), the Suzhou Science and Technology Development Project (SYSD2018144), and the Changshu Science and Technology Program Social Development Project (CS202116).

Editorial note

&This corresponding author has a verified history of publications using a personal email address for correspondence.

REFERENCES

1. Siegel RL, Miller KD, Wagle NS, Jemal A. Cancer statistics, 2023. *CA Cancer J Clin.* 2023; 73:17–48. <https://doi.org/10.3322/caac.21763> PMID:[36633525](https://pubmed.ncbi.nlm.nih.gov/36633525/)
2. Xia C, Dong X, Li H, Cao M, Sun D, He S, Yang F, Yan X, Zhang S, Li N, Chen W. Cancer statistics in China and United States, 2022: profiles, trends, and determinants. *Chin Med J (Engl).* 2022; 135:584–90. <https://doi.org/10.1097/CM9.0000000000002108> PMID:[35143424](https://pubmed.ncbi.nlm.nih.gov/35143424/)
3. Yeoh KG, Tan P. Mapping the genomic diaspora of gastric cancer. *Nat Rev Cancer.* 2022; 22:71–84. <https://doi.org/10.1038/s41568-021-00412-7> PMID:[34702982](https://pubmed.ncbi.nlm.nih.gov/34702982/)
4. Chen W, Zheng R, Baade PD, Zhang S, Zeng H, Bray F, Jemal A, Yu XQ, He J. Cancer statistics in China, 2015. *CA Cancer J Clin.* 2016; 66:115–32. <https://doi.org/10.3322/caac.21338> PMID:[26808342](https://pubmed.ncbi.nlm.nih.gov/26808342/)
5. Hojnik M, Šuster NK, Smrkolj Š, Sisinger D, Grazio SF, Verdenik I, Rižner TL. AKR1B1 as a Prognostic Biomarker of High-Grade Serous Ovarian Cancer. *Cancers (Basel).* 2022; 14:809. <https://doi.org/10.3390/cancers14030809> PMID:[35159076](https://pubmed.ncbi.nlm.nih.gov/35159076/)
6. Dai T, Ye L, Yu H, Li K, Li J, Liu R, Lu X, Deng M, Li R, Liu W, Yang Y, Wang G. Regulation Network and Prognostic Significance of Aldo-Keto Reductase (AKR) Superfamily Genes in Hepatocellular Carcinoma. *J Hepatocell Carcinoma.* 2021; 8:997–1021. <https://doi.org/10.2147/JHC.S323743> PMID:[34513744](https://pubmed.ncbi.nlm.nih.gov/34513744/)
7. Tanawattanasuntorn T, Rattanaburee T, Thongpanchang T, Graidist P. *Trans*-(±)-Kusunokinin Binding to AKR1B1 Inhibits Oxidative Stress and Proteins Involved in Migration in Aggressive Breast

- Cancer. *Antioxidants (Basel)*. 2022; 11:2347.
<https://doi.org/10.3390/antiox11122347>
PMID:36552555
8. Saeed A, Ejaz SA, Sarfraz M, Tamam N, Siddique F, Riaz N, Qais FA, Chtita S, Iqbal J. Discovery of Phenylcarbamoylazine-1,2,4-Triazole Amides Derivatives as the Potential Inhibitors of Aldo-Keto Reductases (AKR1B1 & AKR1B10): Potential Lead Molecules for Treatment of Colon Cancer. *Molecules*. 2022; 27:3981.
<https://doi.org/10.3390/molecules27133981>
PMID:35807227
 9. Zhang KR, Zhang YF, Lei HM, Tang YB, Ma CS, Lv QM, Wang SY, Lu LM, Shen Y, Chen HZ, Zhu L. Targeting AKR1B1 inhibits glutathione de novo synthesis to overcome acquired resistance to EGFR-targeted therapy in lung cancer. *Sci Transl Med*. 2021; 13:eabg6428.
<https://doi.org/10.1126/scitranslmed.abg6428>
PMID:34613810
 10. Cao M, Tian Z, Zhang L, Liu R, Guan Q, Jiang J. Genetic association of AKR1B1 gene polymorphism rs759853 with diabetic retinopathy risk: A meta-analysis. *Gene*. 2018; 676:73–8.
<https://doi.org/10.1016/j.gene.2018.07.014>
PMID:30201105
 11. Wu TT, Chen YY, Ho CY, Yeh TC, Sun GC, Tseng CJ, Cheng PW. 3H-1,2-Dithiole-3-Thione Protects Lens Epithelial Cells against Fructose-Induced Epithelial-Mesenchymal Transition via Activation of AMPK to Eliminate AKR1B1-Induced Oxidative Stress in Diabetes Mellitus. *Antioxidants (Basel)*. 2021; 10:1086.
<https://doi.org/10.3390/antiox10071086>
PMID:34356319
 12. Reddy KA, Kumar PU, Srinivasulu M, Triveni B, Sharada K, Ismail A, Reddy GB. Overexpression and enhanced specific activity of aldoketo reductases (AKR1B1 & AKR1B10) in human breast cancers. *Breast*. 2017; 31:137–43.
<https://doi.org/10.1016/j.breast.2016.11.003>
PMID:27855345
 13. Duan T, Zhou D, Yao Y, Shao X. Corrigendum: The Association of Aberrant Expression of FGF1 and mTOR-S6K1 in Colorectal Cancer. *Front Oncol*. 2021; 11:792453.
<https://doi.org/10.3389/fonc.2021.792453>
PMID:34760712
 14. Yao Y, Zhou D, Shi D, Zhang H, Zhan S, Shao X, Sun K, Sun L, Wu G, Tian K, Zhu X, He S. GLI1 overexpression promotes gastric cancer cell proliferation and migration and induces drug resistance by combining with the AKT-mTOR pathway. *Biomed Pharmacother*. 2019; 111:993–1004.
<https://doi.org/10.1016/j.biopha.2019.01.018>
PMID:30841479
 15. Jiang Q, Zhang X, Dai X, Han S, Wu X, Wang L, Wei W, Zhang N, Xie W, Guo J. S6K1-mediated phosphorylation of PDK1 impairs AKT kinase activity and oncogenic functions. *Nat Commun*. 2022; 13:1548.
<https://doi.org/10.1038/s41467-022-28910-8>
PMID:35318320
 16. Zhou D, Yao Y, Zong L, Zhou G, Feng M, Chen J, Liu G, Chen G, Sun K, Yao H, Liu Y, Shi X, Zhang W, et al. TBK1 Facilitates GLUT1-Dependent Glucose Consumption by suppressing mTORC1 Signaling in Colorectal Cancer Progression. *Int J Biol Sci*. 2022; 18:3374–89.
<https://doi.org/10.7150/ijbs.70742>
PMID:35637944
 17. Kopecky K, Monton O, Rosman L, Johnston F. Palliative interventions for patients with advanced gastric cancer: a systematic review. *Chin Clin Oncol*. 2022; 11:47.
<https://doi.org/10.21037/cco-22-102>
PMID:36632980
 18. Hall CE, Maegawa F, Patel AD, Lin E. Management of Gastric Cancer. *Am Surg*. 2023; 89:2713–20.
<https://doi.org/10.1177/00031348221148359>
PMID:36609184
 19. Zhao M, Yang Y, Nian Q, Shen C, Xiao X, Liao W, Zheng Q, Zhang G, Chen N, Gong D, Tang J, Wen Y, Zeng J. Phytochemicals and mitochondria: Therapeutic allies against gastric cancer. *Phytotherapy*. 2023; 110:154608.
<https://doi.org/10.1016/j.phymed.2022.154608>
PMID:36586205
 20. Siri G, Yazdani O, Esbati R, Akhavanfar R, Asadi F, Adili A, Ebrahimzadeh F, Hosseini SME. A comprehensive review of the role of lncRNAs in gastric cancer (GC) pathogenesis, immune regulation, and their clinical applications. *Pathol Res Pract*. 2023; 241:154221.
<https://doi.org/10.1016/j.prp.2022.154221>
PMID:36563559
 21. Xu J, Xu Y, Ye G, Qiu J. lncRNA-SNHG1 promotes paclitaxel resistance of gastric cancer cells through modulating the miR-216b-5p-hexokinase 2 axis. *J Chemother*. 2022. [Epub ahead of print].
<https://doi.org/10.1080/1120009X.2022.2157618>
PMID:36548909
 22. Kaufman A, Abuqayyas L, Denney WS, Tillman EJ, Rolph T. AKR-001, an Fc-FGF21 Analog, Showed Sustained Pharmacodynamic Effects on Insulin

- Sensitivity and Lipid Metabolism in Type 2 Diabetes Patients. *Cell Rep Med*. 2020; 1:100057.
<https://doi.org/10.1016/j.xcrm.2020.100057>
PMID:[33205064](https://pubmed.ncbi.nlm.nih.gov/33205064/)
23. Penning TM. Aldo-Keto Reductase (AKR) 1C3 inhibitors: a patent review. *Expert Opin Ther Pat*. 2017; 27:1329–40.
<https://doi.org/10.1080/13543776.2017.1379503>
PMID:[28895472](https://pubmed.ncbi.nlm.nih.gov/28895472/)
24. Dieter C, Lemos NE, de Faria Corrêa NR, Pellenz FM, Canani LH, Crispim D, Bauer AC. The A allele of the rs759853 single nucleotide polymorphism in the *AKR1B1* gene confers risk for diabetic kidney disease in patients with type 2 diabetes from a Brazilian population. *Arch Endocrinol Metab*. 2022; 66:12–8.
<https://doi.org/10.20945/2359-3997000000432>
PMID:[35029856](https://pubmed.ncbi.nlm.nih.gov/35029856/)
25. Kaur N, Vanita V. Association of aldose reductase gene (*AKR1B1*) polymorphism with diabetic retinopathy. *Diabetes Res Clin Pract*. 2016; 121:41–8.
<https://doi.org/10.1016/j.diabres.2016.08.019>
PMID:[27640118](https://pubmed.ncbi.nlm.nih.gov/27640118/)
26. Saraswathy R, Anand S, Kunnumpurath SK, Kurian RJ, Kaye AD, Vadivelu N. Chromosomal Aberrations and Exon 1 Mutation in the *AKR1B1* Gene in Patients with Diabetic Neuropathy. *Ochsner J*. 2014; 14:339–42.
PMID:[25249799](https://pubmed.ncbi.nlm.nih.gov/25249799/)
27. Taskoparan B, Seza EG, Demirkol S, Tuncer S, Stefek M, Gure AO, Banerjee S. Opposing roles of the aldose reductases *AKR1B1* and *AKR1B10* in colorectal cancer. *Cell Oncol (Dordr)*. 2017; 40:563–78.
<https://doi.org/10.1007/s13402-017-0351-7>
PMID:[28929377](https://pubmed.ncbi.nlm.nih.gov/28929377/)
28. Zhang G, Dong K, Liu J, Zhou W. Prognosis and tumor immune microenvironment of patients with gastric cancer by a novel senescence-related signature. *Medicine (Baltimore)*. 2022; 101:e30927.
<https://doi.org/10.1097/MD.00000000000030927>
PMID:[36221394](https://pubmed.ncbi.nlm.nih.gov/36221394/)
29. Li Q, Wang R, Yang Z, Li W, Yang J, Wang Z, Bai H, Cui Y, Tian Y, Wu Z, Guo Y, Xu J, Wen L, et al. Molecular profiling of human non-small cell lung cancer by single-cell RNA-seq. *Genome Med*. 2022; 14:87.
<https://doi.org/10.1186/s13073-022-01089-9>
PMID:[35962452](https://pubmed.ncbi.nlm.nih.gov/35962452/)
30. Luo L, Chen C, He H, Cai M, Ling C. Silencing of Long Non-Coding RNA (*LncRNA*) Non-Coding RNA Activated by DNA Damage (*NORAD*) Inhibits Proliferation, Invasion, Migration, and Promotes Apoptosis of Glioma Cells via Downregulating the Expression of *AKR1B1*. *Med Sci Monit*. 2020; 26:e922659.
<https://doi.org/10.12659/MSM.922659>
PMID:[32778640](https://pubmed.ncbi.nlm.nih.gov/32778640/)
31. Ji J, Xu MX, Qian TY, Zhu SZ, Jiang F, Liu ZX, Xu WS, Zhou J, Xiao MB. The *AKR1B1* inhibitor epalrestat suppresses the progression of cervical cancer. *Mol Biol Rep*. 2020; 47:6091–103.
<https://doi.org/10.1007/s11033-020-05685-z>
PMID:[32761301](https://pubmed.ncbi.nlm.nih.gov/32761301/)
32. de Groot JS, Moelans CB, Elias SG, Jo Fackler M, van Domselaar R, Suijkerbuijk KP, Witkamp AJ, Sukumar S, van Diest PJ, van der Wall E. DNA promoter hypermethylation in nipple fluid: a potential tool for early breast cancer detection. *Oncotarget*. 2016; 7:24778–91.
<https://doi.org/10.18632/oncotarget.8352>
PMID:[27028854](https://pubmed.ncbi.nlm.nih.gov/27028854/)
33. Torres-Mena JE, Salazar-Villegas KN, Sánchez-Rodríguez R, López-Gabiño B, Del Pozo-Yauner L, Arellanes-Robledo J, Villa-Treviño S, Gutiérrez-Nava MA, Pérez-Carreón JI. Aldo-Keto Reductases as Early Biomarkers of Hepatocellular Carcinoma: A Comparison Between Animal Models and Human HCC. *Dig Dis Sci*. 2018; 63:934–44.
<https://doi.org/10.1007/s10620-018-4943-5>
PMID:[29383608](https://pubmed.ncbi.nlm.nih.gov/29383608/)
34. Tammali R, Ramana KV, Singhal SS, Awasthi S, Srivastava SK. Aldose reductase regulates growth factor-induced cyclooxygenase-2 expression and prostaglandin E2 production in human colon cancer cells. *Cancer Res*. 2006; 66:9705–13.
<https://doi.org/10.1158/0008-5472.CAN-06-2105>
PMID:[17018629](https://pubmed.ncbi.nlm.nih.gov/17018629/)
35. Ramana KV, Tammali R, Srivastava SK. Inhibition of aldose reductase prevents growth factor-induced G1-S phase transition through the AKT/phosphoinositide 3-kinase/E2F-1 pathway in human colon cancer cells. *Mol Cancer Ther*. 2010; 9:813–24.
<https://doi.org/10.1158/1535-7163.MCT-09-0795>
PMID:[20354121](https://pubmed.ncbi.nlm.nih.gov/20354121/)
36. Golden E, Rashwan R, Woodward EA, Sgro A, Wang E, Sorolla A, Waryah C, Tie WJ, Cuyàs E, Ratajska M, Kardaś I, Kozłowski P, Johnstone EKM, et al. The oncogene *AAMDC* links PI3K-AKT-mTOR signaling with metabolic reprogramming in estrogen receptor-positive breast cancer. *Nat Commun*. 2021; 12:1920.
<https://doi.org/10.1038/s41467-021-22101-7>
PMID:[33772001](https://pubmed.ncbi.nlm.nih.gov/33772001/)
37. Zhou D, Jiang L, Jin L, Yao Y, Wang P, Zhu X. Glucose Transporter-1 Cooperating with AKT Signaling Promote Gastric Cancer Progression. *Cancer Manag Res*. 2020; 12:4151–60.
<https://doi.org/10.2147/CMAR.S251596>
PMID:[32581586](https://pubmed.ncbi.nlm.nih.gov/32581586/)

38. Yao Y, Yang X, Sun L, Sun S, Huang X, Zhou D, Li T, Zhang W, Abumrad NA, Zhu X, He S, Su X. Fatty acid 2-hydroxylation inhibits tumor growth and increases sensitivity to cisplatin in gastric cancer. *EBioMedicine*. 2019; 41:256–67.
<https://doi.org/10.1016/j.ebiom.2019.01.066>
PMID:[30738828](https://pubmed.ncbi.nlm.nih.gov/30738828/)
39. Khayami R, Hashemi SR, Kerachian MA. Role of aldo-keto reductase family 1 member B1 (AKR1B1) in the cancer process and its therapeutic potential. *J Cell Mol Med*. 2020; 24:8890–902.
<https://doi.org/10.1111/jcmm.15581>
PMID:[32633024](https://pubmed.ncbi.nlm.nih.gov/32633024/)
40. Shukla K, Sonowal H, Saxena A, Ramana KV, Srivastava SK. Aldose reductase inhibitor, fidarestat regulates mitochondrial biogenesis via Nrf2/HO-1/AMPK pathway in colon cancer cells. *Cancer Lett*. 2017; 411:57–63.
<https://doi.org/10.1016/j.canlet.2017.09.031>
PMID:[28986187](https://pubmed.ncbi.nlm.nih.gov/28986187/)